

Article

Spatial and Temporal Evolution of Sowing and the Onset of the Rainy Season in a Region of Large Agricultural Expansion in Brazil

Humberto Paiva Fonseca , Gabrielle Ferreira Pires * and Livia Maria Brumatti 

Department of Agricultural Engineering, Federal University of Viçosa, Viçosa 36570-900, Brazil; humberto.fonseca@ufv.br (H.P.F.); livia.brumatti@ufv.br (L.M.B.)

* Correspondence: gabrielle.pires@ufv.br; Tel.: +55-(31)-3612-4041

Abstract: In order to assist in high-yield agricultural management in multiple cropping systems, it is essential to understand the link between the rainy season onset and crops sowing dates, since it considerably affects the management, yield and output. We built crop calendars derived from remote sensing products and investigated the link between sowing dates and the onset of the rainy season in irrigated and rainfed agriculture in Western Bahia, a new and important agricultural frontier in Brazilian Cerrado. Crop sowing dates were obtained from green-up dates from 2001 to 2019. Rainy season onset dates were determined using CHIRPS daily precipitation data. Results indicate that sowing occurs from 26 October to 15 November and the rainy season starts from 17 to 27 October. Rainfed sowing dates are strongly correlated to rainy season onset and are particularly affected in years where rains are delayed. Sowing dates in irrigated pixels occur up to 25 days earlier than rainfed and are not correlated to rainy season onset. Irrigated farms are sowing earlier and in a shorter window than rainfed, with a stronger resilience in years where rains are delayed, and have adapted their sowing operation towards a more intensive agriculture and efficient water use during the rainy season.

Keywords: Western Bahia; MODIS; sowing dates; irrigation; rainfed agriculture



Citation: Fonseca, H.P.; Pires, G.F.; Brumatti, L.M. Spatial and Temporal Evolution of Sowing and the Onset of the Rainy Season in a Region of Large Agricultural Expansion in Brazil. *Agronomy* **2022**, *12*, 1679. <https://doi.org/10.3390/agronomy12071679>

Academic Editors: Maria-Paz Diago and Riccardo Dainelli

Received: 1 June 2022
Accepted: 13 July 2022
Published: 15 July 2022

Publisher's Note: MDPI stays neutral with regard to jurisdictional claims in published maps and institutional affiliations.



Copyright: © 2022 by the authors. Licensee MDPI, Basel, Switzerland. This article is an open access article distributed under the terms and conditions of the Creative Commons Attribution (CC BY) license (<https://creativecommons.org/licenses/by/4.0/>).

1. Introduction

The importance of the agriculture sector to the Brazilian economy is prominent. In 2020/2021, this sector contributed ~22% of gross domestic product (GDP), with expectations of a 2% increase in 2022 [1]. During the same period, soybean (*Glycine max*) exports increased by 21% compared to 2016/2017. Other crops also contributed positively to Brazil's export balance, with cotton and maize standing out [1].

Brazil is currently amongst the world's greatest exporter of soybean, maize (*Zea mays*) and cotton (*Gossypium hirsutum* L.), with exports increasing mostly as a result of technological advancements and mechanization, especially in the Cerrado [2]. The MATOPIBA region (acronym for the states of Maranhão, Tocantins, Piauí and Bahia), located in the Cerrado, is one of the most recent agricultural frontiers, with a high yield of soybean, cotton and maize crops, reaching a national record of 7.4 million tons in the 2016/2017 harvest [3]. The importance of MATOPIBA is related to the rapid growth of agriculture in the western part of Bahia state (hereafter called Western Bahia, WB), where the average maize yield increased to 10.5 ton.ha⁻¹ in the 2020/2021 harvest, with a potential output of 11 ton.ha⁻¹ predicted for the year 2023 due to investments in high technology and irrigation [4]. In addition, high productivity levels were achieved in the cultivation of soybeans, with 4 ton.ha⁻¹ [4], and cotton, with 4.5 ton.ha⁻¹, in the 2021/2022 harvest [4].

Western Bahia continues to stand out for its worldwide market position, with approximately 40% of cotton output, or 600,000 tons, exported to Asian nations (China, Indonesia, Bangladesh, and Vietnam), and 60% of soybean production, or 3.18 million tons, exported

to China and the Netherlands [4]. The high production and export rates achieved by the region could be partly explained by the adoption of double cropping systems, where farmers sow a second crop (maize or cotton) in the middle of the rainy season after sowing soybeans in the beginning of the rainy season [5,6]; and the wide adoption of irrigation, which increased its area by around 800% from 1990 to 2020 [7].

Double cropping systems are favored in regions with a high annual precipitation rate, a long rainy season (>200 days), and a low variability in the rainy season onset [5,6,8]. The viability of double cropping depends on farmers successfully sowing soybeans right at the beginning of the rainy season. A delay in rainy season onset retards the sowing operation of the first crop, leaving less time for the second crop to grow before rainy season ceases. Irrigated farms may have strategic advantages over rainfed farms, but its success depends on the availability of water in rivers at the end of the dry season. The rivers in WB are regulated by the Urucua aquifer, which showed a groundwater level drawdown of up to 5 m from 2011 to 2015 [9]. In addition, rainfall and rivers discharge are reducing in the region [10], creating a potential to cause conflicts over water use during the dry season.

Recent studies indicate that the rainy season is starting later and shortening in central Brazil [11–14] due to both climate change and widespread Amazon and Cerrado deforestation. This worrying scenario is projected to intensify in the future [15], with disastrous potential impacts in case local farmers fail to adapt [5,6].

As sowing dates have a significant impact on the double cropping viability and production, historical sowing calendars are needed to properly assess the effects of a delayed rainy season onset on agriculture. However, information on sowing dates in Brazil are restricted to the last decade and are not spatialized, especially for WB, hampering the evaluation of the impacts of rainy season delays on the regional agricultural calendar and the investigation of potential adaptation measures.

Despite the difficulty in determining sowing dates for large areas in Brazil, recent studies achieved favorable results in the state of Mato Grosso, which has significant implications for the national and international agricultural scenario [14]. However, sowing calendars for WB are still missing.

Fortunately, several recent studies have designed methods that enable the identification of sowing dates based on the determination of phenological phases in a dense time series of vegetative indices acquired from orbital images [16–18]. Even though satellite imagery might show some limitations for agriculture monitoring due to temporal resolution, sensors such as the Moderate Resolution Imaging Spectroradiometer (MODIS) provide precise temporal crop information for regions such as WB, with large-scale monoculture on flat terrains.

In this study, we aim to build crop calendars and evaluate the relationship between crop sowing dates and rainy season onset in irrigated and rainfed agriculture in Western Bahia from 2001 to 2019. We believe that it provides important and strategic information for the adaptation of double cropping systems to climate change.

2. Materials and Methods

We estimated crop sowing dates using the normalized difference vegetation index (NDVI) and daily temperature data from MODIS. Rainy season onset dates were determined using daily precipitation data from Climate Hazards Group InfraRed Precipitation with Stations data (CHIRPS [19]) and the anomalous accumulation method [20]. In this study, we distinguished rainfed and irrigated croplands based on land use and land cover data from Pimenta et al. [7], from 2001 to 2019 (Figure S1 and available at <http://obahia.dea.ufv.br/>; accessed on 1 June 2022).

In summary, we began by filtering any noise from the NDVI time series and evaluating a variety of interpolators (Figure 1, first step). We determined the sowing dates from green-up date and air temperature (Figure 1, second step). Finally, we sought to establish a relationship between the sowing dates and the rainy season onset dates (Figure 1, third step).

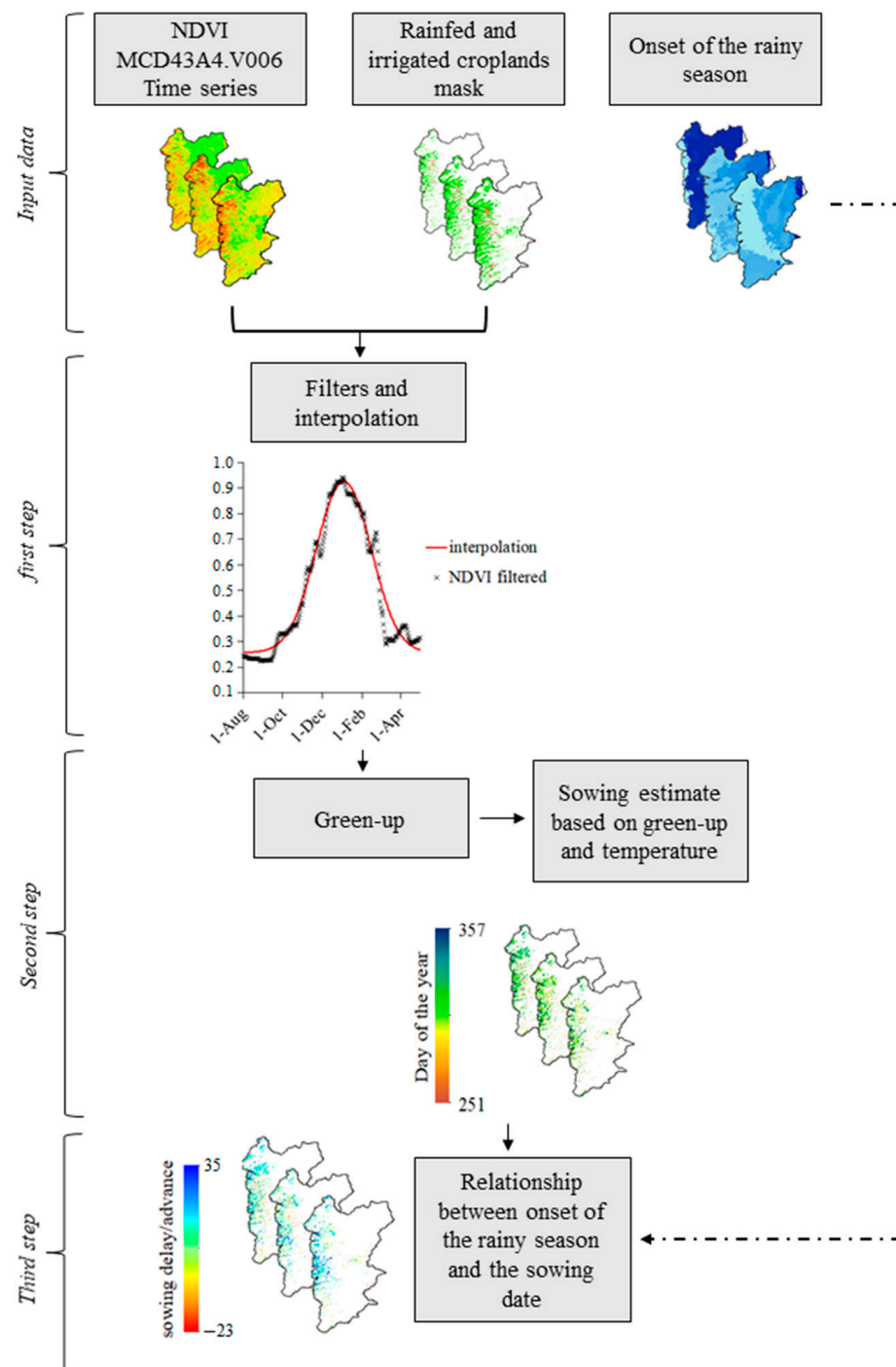


Figure 1. Steps for the determination of sowing and rainy season onset dates in Western Bahia.

2.1. Study Area

Western Bahia (Figure 2) covers approximately 130,000 km² and is part of the most recent agricultural frontier in the Brazilian Cerrado biome, called MATOPIBA. The region is characterized by rapid expansion followed by mechanization and intensification, resulting in high yields of crops such as beans (*Phaseolus vulgaris*), cassava (*Manihot esculenta*), coffee (*Coffea canephora*), cotton (*Gossypium hirsutum* L.), maize (*Zea mays*), rice (*Oryza sativa*) and soybeans (*Glycine max*) [10,17,21].

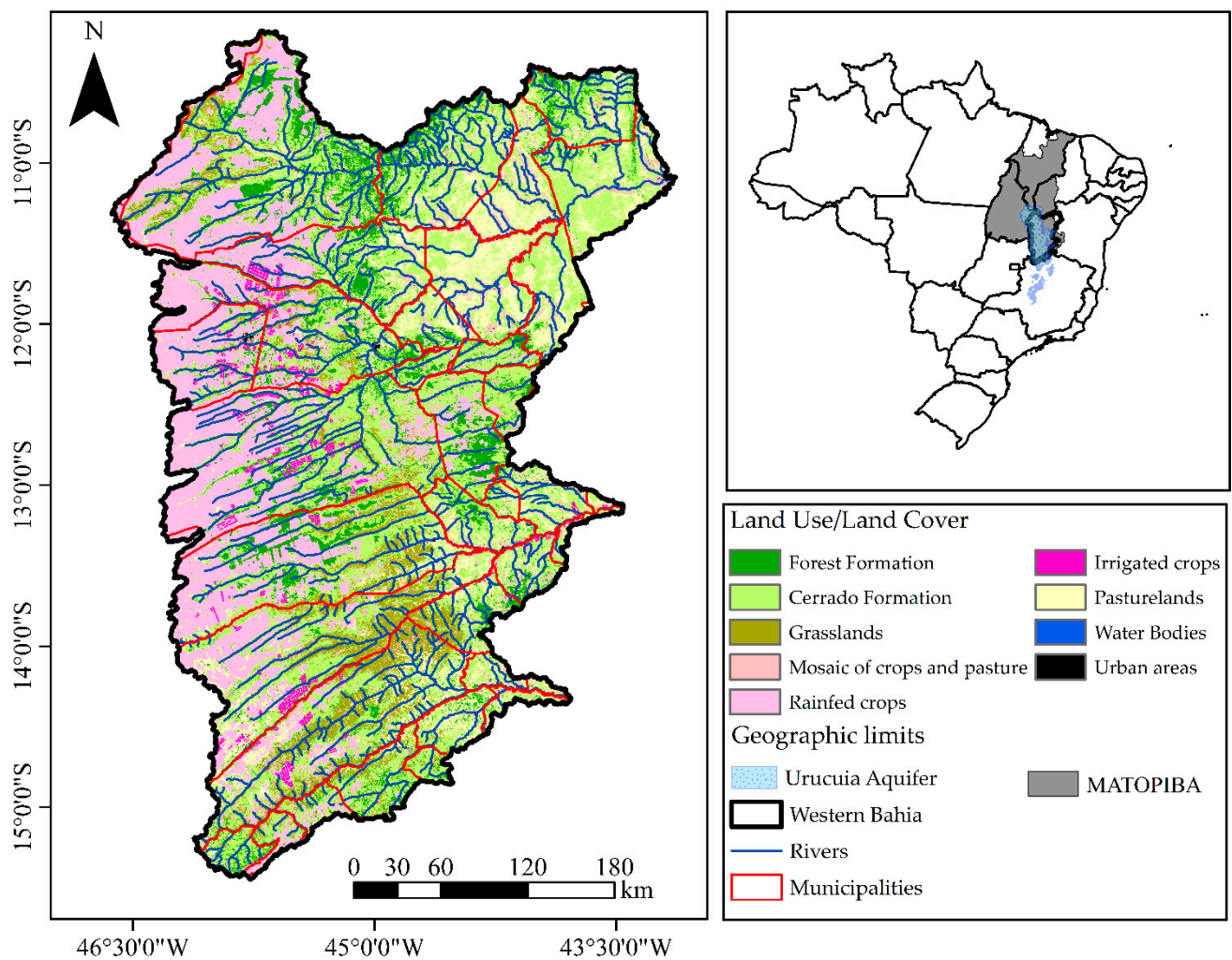


Figure 2. Location and land use/land cover for Western Bahia in 2019, according to Pimenta et al. [7] and available at: <http://obahia.dea.ufv.br/> (accessed on 1 June 2022).

Western Bahia stands out from other agricultural regions in Brazil due to its rapid and recent expansion, especially irrigated lands. In summary, 100,000 km² are dedicated to rainfed agriculture and 2000 km² are occupied by irrigation systems (mainly center pivots). Approximately 85% of the farms in the region have more than 5 km² of land [7].

Part of the high yields observed in the region can be attributed to the favorable climatic and geographical conditions. Rainfall in WB typically ranges from 0–10 mm.month⁻¹ in the driest months (June, July and August) and approximately 150–200 mm.month⁻¹ in the wettest months (December and January) [10]. The average annual rainfall in the extreme west is 1400 mm, gradually falling to 800 mm in the east, on the border with the Caatinga biome [3]. The region has flat terrain suitable for the use of large agricultural machinery.

2.2. Remote Sensing Data and NDVI Interpolators

NDVI data were derived from MODIS MCD43A4.V006 product, which shows long-term stability and widespread application in agricultural phenology studies [16,22]. MCD43A4.V006 has a spatial resolution of 500 m, seven spectral bands ranging from visible to near-infrared wavelengths and nadir-adjusted reflectance (NBAR) scenes generated by daily bidirectional reflectance distribution function (BRDF) centered at midday solar and generated from short-term resampling (16 days) by an algorithm based on the inversion of radiative transfer models present in the V006 [22,23].

Approximately 7000 images were acquired from July 2001 to December 2019. Low quality pixels were discarded using MCD43A2 product (incomplete BRDF inversions). Following the acquisition of MCD43A4.V006 images, only pure pixels were selected, or those that contain only one land cover class and are rid of external interference from other spectral signals, such as exposed soil and varied vegetation [24]

We employed a Savitzky–Golay filter to reduce NDVI time series contamination caused by clouds, atmospheric variability, suspended particles and crop management changes [25]. We tested four methods for NDVI interpolation: asymmetric Gaussian, Beck et al. [26], Elmore et al. [27], Gu et al. [28] and Zhang et al. [29].

2.3. Determination of Green-Up Date

Green-up is the first detectable moment of greenness in vegetation after emergence and is a good indicator of a new cycle of plant growth. It can be detected when NDVI exceeds a threshold value, which may vary among crops.

We selected the best NDVI interpolator (Section 2.6) and combined it with six different methods to detect crops green-up dates. Due to the size of the study area and the multiplicity of crops and management practices, a single method would likely not be able to capture the heterogeneity of green-up dates in WB. Therefore, to account for the diverse field conditions in the study area, we assessed multiple methods to detect the green-up dates: the relative threshold method (TRS), the derivative method (DES) and the methods described by White et al. [30], Gu et al. [28] and Zhang et al. [29]. We assumed that a high concordance with field data is achieved when several methods point to the same green-up date pattern. This approach has shown to be effective in capturing green-up dates in different areas, as shown in [14,31–36]. The best green-up methods were determined through the comparison of the sowing dates calculated in this study (Section 2.4) with observed sowing dates, and were therefore applied to the entire region and time-series.

2.3.1. Relative Threshold Method (TRS)

The threshold method (TRS) pinpoints phenophase transitions during crop development by setting threshold NDVI values defined by the user. NDVI thresholds can be absolute or relative (percentage of the NDVI amplitude). Due to the variety of crops and management practices in the study area, we chose to evaluate relative rather than absolute thresholds. We tested the relative thresholds of 20%, 50% and 60% of the NDVI phenological curve amplitude to determine green-up dates.

2.3.2. Derivative Method (DES)

The derivatives of vegetative indices enable the identification of transitions in phenological phases [37]. The derivative method (DES) identifies green-up date as the day when NDVI curve first derivative reaches its maximum value [37]. Likewise, gray-down is identified as the day when NDVI curve first derivative reaches its minimum value.

2.3.3. Gu-Based Method

Gu et al. [28] model the seasonal cycle of vegetation as approximately linear processes using recovery lines for crop emergence (green-up). The recovery line is defined as the line passing through the maximum point of the first derivative of the NDVI phenological curve and with the slope of the peak recovery rate. The peak recovery rate is the maximum value of the first derivative of the NDVI curve [31].

2.3.4. Zhang-Based Method

Zhang et al. [29] explain variations in vegetation phenological phases using the rate of change in logistic functions. Transition dates are defined as the points at which the rate of curvature change in NDVI data approaches local minimum or maximum. The green-up date is determined when the logistic function reaches its first local maximum.

2.4. Determination of Sowing Dates from Green-Up Dates

To determine the sowing date (Doy_{sow}) from green-up date, we applied a modified version of Soltani and Sinclair's [38] biological day computation method as a function of degree-days (Equation (1)). We assumed that, from sowing (Doy_{sow}) until crop emergence ($Doy_{green-up}$), the accumulation of pre-defined temperature units ($CTU_{sow-gup}$) is necessary, according to crop energy requirements. Here, we considered that green-up date is equivalent to the crop emergence date.

$$Doy_{sow} = Doy_{green-up} - \frac{CTU_{sow-gup}}{\sum_{Doy=1}^k DTU} \quad (1)$$

where $CTU_{sow-gup}$ ($^{\circ}C$) is the cumulative temperature units required for the transition from sowing to green-up (here assumed as $70^{\circ}C$), k is the day of the year when the required cumulative temperature units for the transition from sowing to green-up is achieved and DTU is the daily temperature unit ($^{\circ}C \cdot day^{-1}$), calculated as in Equation (2).

$$DTU = (TP1D - TBD) \times tempfun \quad (2)$$

where $TP1D$ is the lowest optimum temperature for crop growth ($21^{\circ}C$), TBD is crop basal temperature ($10^{\circ}C$) and $tempfun$ is the relative development response of crops to temperature (Equation (3)).

$$\begin{aligned} tempfun &= 0 && \text{if } TMP \leq TBD \\ &= (TMP - TBD) / (TP1D - TBD) && \text{if } TBD < TMP < TP1D \\ &= 1 && \text{if } TP1D \leq TMP \leq TP2D \\ &= (TCD - TMP) / (TCD - TP2D) && \text{if } TP2D < TMP < TCD \end{aligned} \quad (3)$$

where TMP is the daily average air temperature ($^{\circ}C$), calculated as the average of four observations (night and day) of MOD11A1 (MODIS-Earth) and MYD11A1 (MODIS-Aqua) products, $TP2D$ is the highest optimal temperature for crop development ($36^{\circ}C$) and TCD is the maximum (ceiling) temperature at which the plant develops ($43^{\circ}C$).

In Brazil, field-level data for irrigated and rainfed agriculture are scarce or non-existent for large territorial extensions. To validate the estimated sowing dates, we compared them with two datasets. The first contains field-level sowing dates in irrigated lands gathered between 2017 and 2019. During this period, a total of 58 center pivots were sown with different crops (soybeans, maize, bean and cotton). Field sowing dates were derived from an irrigation management platform (Valley Scheduling software, Irriger Connect platform) and are described by Santos et al. [39] and Table S2. The second dataset is derived from aggregated sowing windows of the agricultural zoning of climate risk (ZARC), followed by many rainfed farmers to reduce yield losses and to attend to the demands of agricultural credits programs

2.5. Onset of the Rainy Season

The anomalous accumulation method (AA, Equation (4)), developed by Liebmann et al. [40] and modified by Arvor et al. [20], was used to determine the rainy season onset in the study area. This method is based on the premise that crops cannot be exposed to extended dryness following the onset of the rainy season. The lowest and highest values of the AA series correspond to the rainy season onset and cessation dates, respectively.

$$AA(t) = \sum_{n=1}^t [R(n) - R_{ref}] \quad (4)$$

where R_{ref} is the lowest amount of water required by crops during their early phenological phases, here assumed as $2.5 \text{ mm} \cdot \text{day}^{-1}$ [5], and $R(n)$ denotes daily precipitation ($\text{mm} \cdot \text{day}^{-1}$).

Precipitation data from July 2000 to December 2020 were derived from the Climate Hazards Group InfraRed Precipitation with Stations (CHIRPS) product, with high temporal (daily) and spatial (5 km) resolution [19,41].

2.6. Statistical Analysis

The best NDVI interpolator method was determined as the one with the highest number of pixels that met the following conditions when compared to the observed data: Pearson correlation ($R \geq 0.95$); root-mean-square error ($RMSE \leq 0.5$); Nash–Sutcliffe efficiency ($NSE \geq 0.85$).

Tendencies in sowing dates and rainy season onset were assessed through Mann–Kendall test ($\alpha = 5\%$). Trend magnitudes were determined by Sen’s slope and possible change points in time-series were assessed by Pettitt’s test ($\alpha = 5\%$). The relationship between sowing and rainy season onset dates was assessed through the pixel-by-pixel correlation coefficient (only pixels cultivated for more than 10 years were considered).

3. Results

3.1. NDVI Interpolation and Green-Up Determination Methods

For all the NDVI interpolation methods tested, the southern portion of the region had the lowest average Pearson correlation coefficient (Figure S2A–E), ranging from 0.85 to 0.90, with a standard deviation of 0.05 to 0.15. A similar pattern was found for the Nash–Sutcliffe efficiency coefficient (Figure S2K–O), ranging between 0.6 and 0.8 in the southern portion of the region. The region’s extreme west exhibited the highest Pearson correlation coefficient ($R: 0.90$; standard deviation: 0.10) and a higher Nash–Sutcliffe model efficiency ($NSE: 0.8$; standard deviation: 0.2). The improved results for the western part of the region might be related to the higher planting density, which results in a lower daily fluctuation of NDVI.

In general, the asymmetric Gaussian and Gu et al.’s [28] NDVI interpolation methods showed the best adjustment to observed NDVI data. Indeed, Gu et al.’s method found the best agreement with observed data, with 31% of the study area having phenological curves with an R and NSE higher than 0.95 and 0.90, respectively (Figures S3 and S4), and was therefore selected as the NDVI curve interpolation method in this study.

Based on the NDVI curves calculated from Gu et al.’s [28] method, the green-up dates determined by the relative threshold (TRS, 20% and 50%) and the derivatives (DES) methods had the best green-up and sowing dates estimation compared to field data, and, therefore, the estimated sowing dates for each pixel throughout the time series were calculated as the average of these methods. Estimated dates in irrigated lands agree with observed dates, with $R^2 \approx 0.99$ and an average error of approximately 3 days (Figure 3).

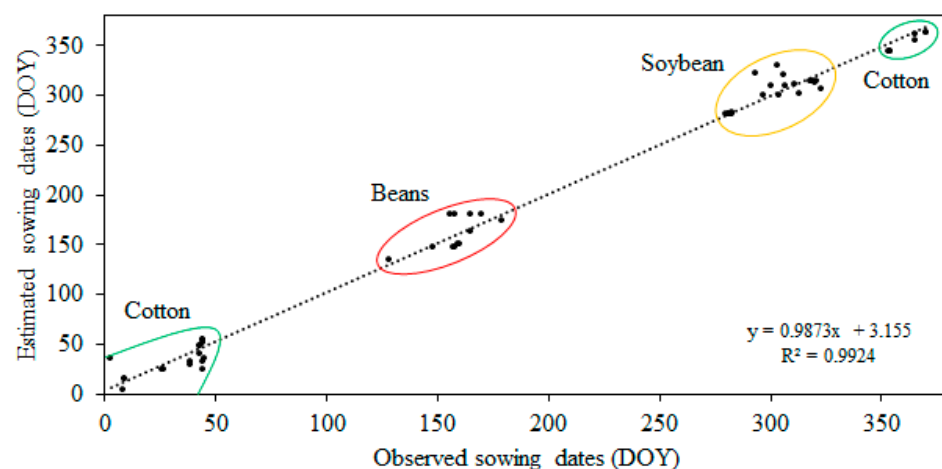


Figure 3. NDVI-derived sowing dates versus field sowing dates.

To test our results for rainfed areas, we compared estimated sowing dates to ZARC sowing windows (Table S1). We selected the sowing window of short-cycle soybean cultivars (Group I) for each municipality in WB, since soybean dominates as the first crop in multiple cropping systems in the region. Estimated sowing dates agree with the lower limit of the ZARC sowing window, which matches the farmers' preference to sow as early as possible in the beginning of the agricultural calendar, especially in multiple cropping systems.

3.2. Sowing Dates

First crop sowing dates in rainfed pixels varied from 26 October to 15 November (Figure 4T), with the region's historical average on 29 October and median on 1 November. In general, rainfed sowing dates occur approximately 15 days earlier in eastern (~44° W) and southern (~15° S) WB than in the western and northern parts of the region (Figures 4T and 5).

Two years were atypical and stood out in the time-series: 2004 and 2007 (Figures 4D,G and 5). In 2004 (Figures 4D and 5), more than half of the total agricultural land's first crop was sown between December 5th and January 14th, 40 to 60 days later than the regional historical average. In 2007 (Figure 4G), on the other hand, first crop sowing occurred approximately 30 to 40 days before the historical average in the central and eastern portions of the region, taking place between September 16th and October 6th. Despite this fact, 50% of the region was sown from 7 October to 27, especially in the extreme western portion of WB. In 2004, a long dry spell and subsequent delay in the rainy season onset had a direct effect on the rainfed sowing date, which varied, on average, between December 5th and January 14th. The delay in the rainfed sowing operation in 2004 may have been caused by a significant warming of the Pacific and North Atlantic oceans. The warmer Pacific resulted in an El Niño event and a reduction in precipitation throughout the Northeast of Brazil that prompted farmers in MATOPIBA to delay planting dates, particularly for soybeans [42,43]. The warmer North Atlantic caused a shift in the intertropical convergence zone (ITCZ) northward of its climatological position from 21 September to 5 October [44], intensifying the rainfall reduction in the region [45].

Rainfed second crop sowing dates varied from 7 March to 12 May—a shorter sowing window than the first crop—with the regional average on March 30th and median on April 15th (Figure 5). The delay and advance in first crop sowing dates in the atypical years of 2004 and 2007, respectively, did not impact the second crop sowing operation with the same intensity. Finally, no significant trend in the median of rainfed sowing dates, for both first and second crops, was detected during the study period (Table 1).

Table 1. Tendency in rainy season onset and sowing dates for Western Bahia.

Onset/Sowing Dates	Tendency (Days·Year ⁻¹)	p-Value	Change Point
Rainy season	0.500	0.483	-
Rainfed, first crop	-0.500	0.139	-
Rainfed, second crop	-0.167	0.226	-
Irrigated, first crop	-0.804 *	0.0358	2013
Irrigated, second crop	-0.364 *	0.0154	2010

* Statistically significant ($\alpha = 0.05$).

First crop sowing dates for irrigated pixels also varied from 26 October to 15 November on average (Figure S5T and Figure 5). As irrigated pixels are concentrated in a small region in western WB (Figure S1), no special spatial pattern emerges like in the rainfed case. However, the temporal distribution of the sowing operation indicates a transformation in the irrigated farmers' behavior. From 2001 to 2013, sowing occurs in a wide temporal window that begins as early as 40 days before and ends up to 40 days after the rainy season onset average. From 2014 on, most of the pixels sow the first crop in a shorter time window and up to 25 days before the rainy season onset average and the rainfed pixels (Figure 5).

Indeed, differently than rainfed, a significant trend both in first and second crop sowing dates was found in irrigated lands: they advance $\sim 0.8 \text{ days.yr}^{-1}$ and $\sim 0.4 \text{ days.yr}^{-1}$ in first and second crops, respectively (Table 1). This tendency translates into ~ 15 and ~ 8 days for the first and second crop, respectively, throughout the study period.

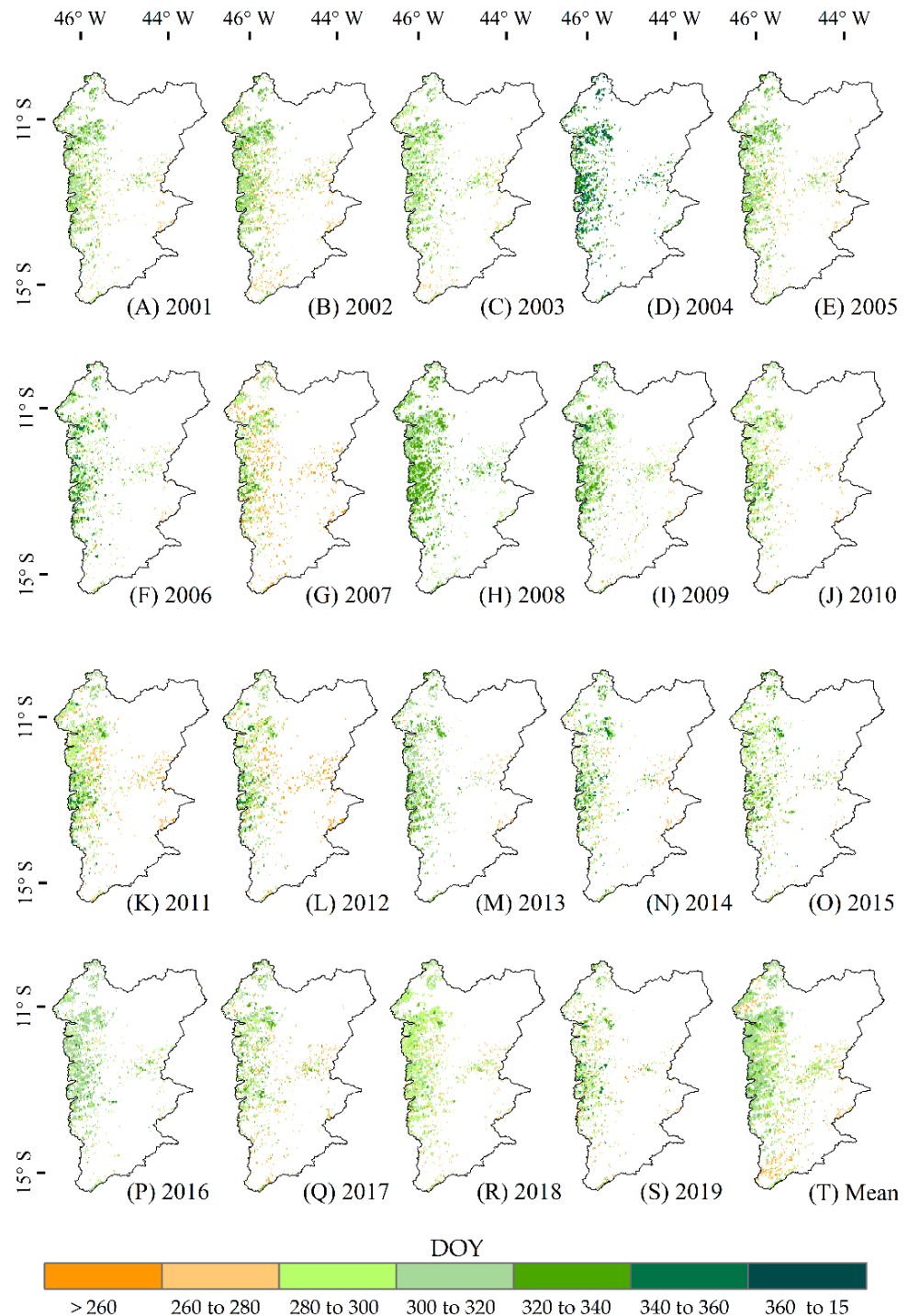


Figure 4. Sowing dates in rainfed areas in Western Bahia from 2001 to 2019 (A–S). Panel (T) shows the average sowing date for each pixel.

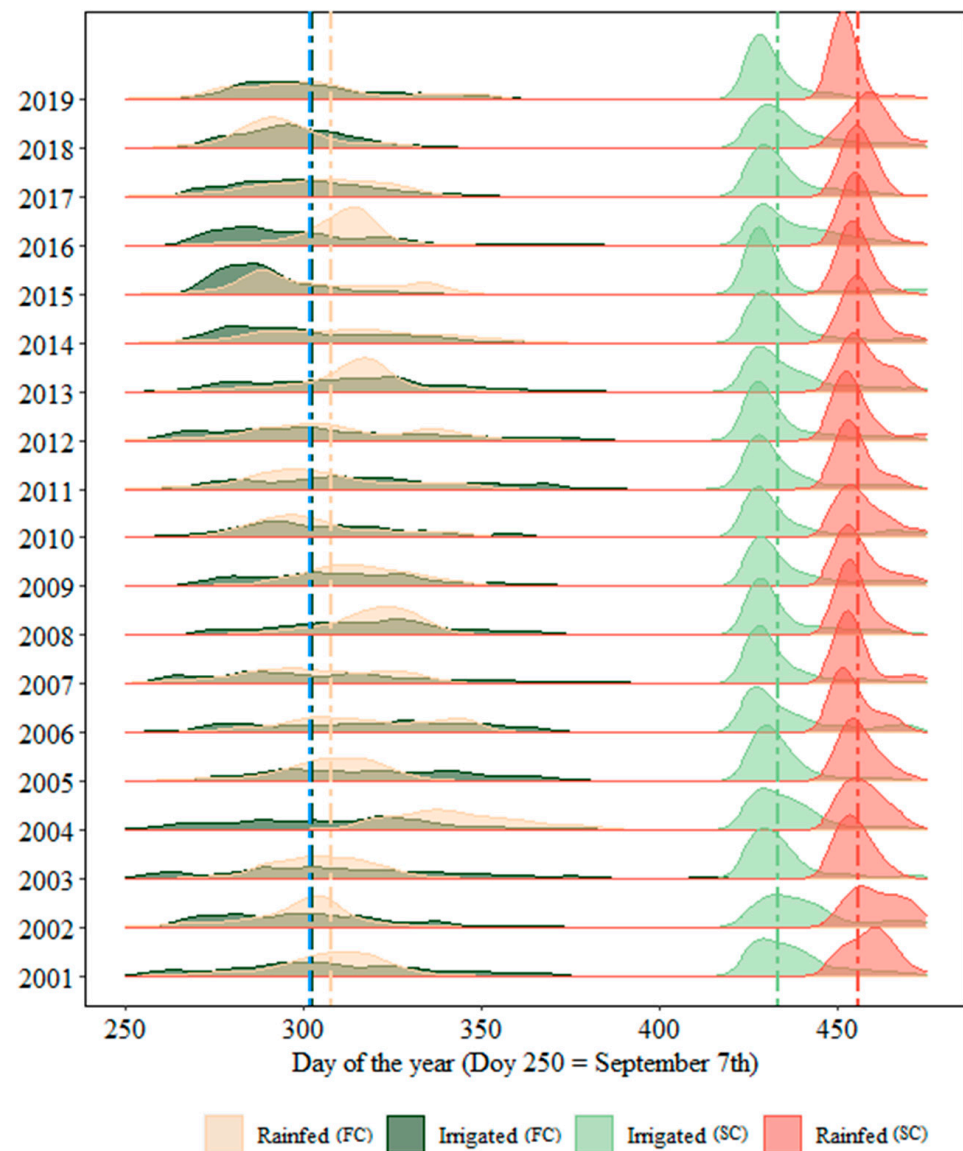


Figure 5. Distribution of rainy season onset, rainfed and irrigated sowing (first and second crop) dates from 2001 to 2019. Lines indicate the median of rainy season onset (blue) and sowing dates for each crop and management practice.

In addition, the difference in the sowing dates for the different management practices is even more evident in years where the rainy season onset was delayed, as in 2004, 2015 and 2016 (Figures 5 and 6). Among these years, 2004 stands out, with irrigated sowing being carried out up to 1.5 months before rainfed systems (Figure 5).

Second crop irrigated pixels were sown between March 24th and April 5th (Figures S5 and S6), a smaller window than the first crop, similarly to the rainfed case. Importantly, second crop irrigated sowing dates occur much earlier than rainfed pixels in all years, a completely distinct behavior to that observed in the first crop sowing operation. In fact, most irrigated pixels are already sown before the rainfed pixels start the sowing operation (Figure 5). The capacity to sow the second crop earlier benefits irrigated lands that sow a third crop (commonly beans) in the same agricultural calendar, which is common in local farms, and lowers costs of irrigation at the end of the rainy season.

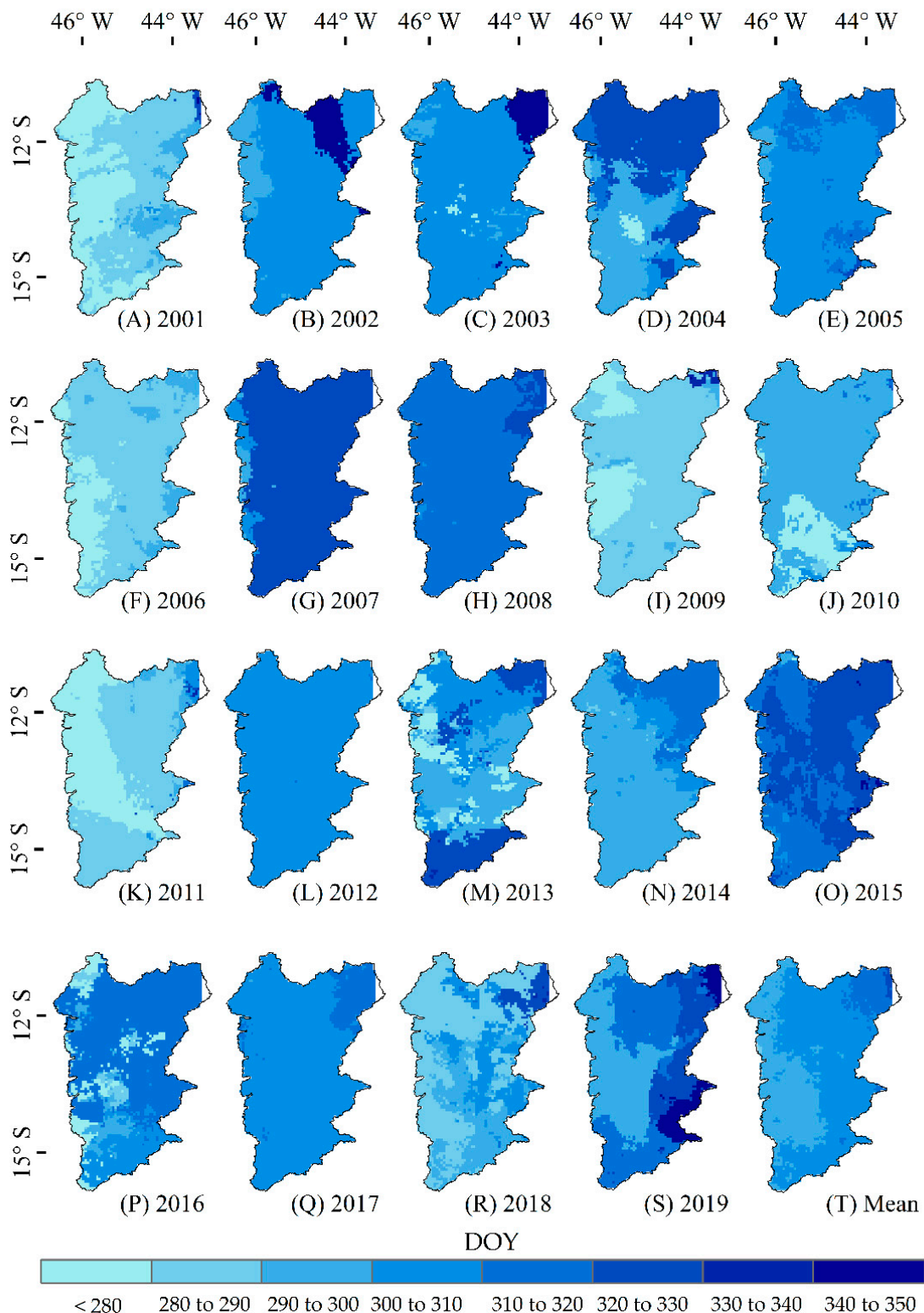


Figure 6. Rainy season onset dates in Western Bahia from 2001 to 2019 (A–S). Panel (T) shows the average onset date for each pixel.

3.3. Onset of the Rainy Season

In general, the rainy season starts earlier in the western part of the region (up until 17 October and later in the east (late November and early December). Therefore, a west–east gradient of rainy season onset is evident in the climatological average (Figure 6T).

However, in 2007, 2008, 2012 and 2017, the rainy season started homogeneously in the study area, with a short delay from the climatological average.

The rainy season started 20 days earlier than the climatological average in 2001, 2006, 2009 and 2011 (Figure 6A,F,I,K). On the other hand, it was delayed by ~30 days in 2004, 2007, 2012 and 2015 (Figure 6G,O).

In addition, in every year after 2012, the rainy season starts later (by the end of October and early November) than the climatological average in the extreme west part of the region, exactly where agriculture is located (Figure S2). Nonetheless, no statistically significant trend was detected in rainy season onset in WB from 2001 to 2019 (Table 1, Figure S8).

3.4. Onset of the Rainy Season and Sowing Dates in Rainfed and Irrigated Systems

Rainfed systems generally sow crops after the onset of the rainy season in most of the area (Figures 4 and 6). The historical and regional median of sowing dates in the rainfed area is 20 days (4 days on average) after rainy season onset. Specifically, in 2001, 2004, 2006, 2009, 2011 and 2013 (Figure 7A,D,F,I,K,M), rainfed pixels were sown up to a month after rainy season onset. After 2014, rainfed systems still sow after rainy season onset, but with shorter delays (Figure 7).

As stated in Section 3.2, 2007 was an atypical year for rainfed systems, where sowing dates occurred much earlier than rainy season onset. In that case, two sowing peaks were observed (Figure 5), and the rainy season onset was delayed expressively throughout the region (Figure 6G). This pattern might indicate an anomalous behavior of rainy season onset, with an initial period of precipitation (47.3 mm) that prompted farmers to start sowing, but followed by a succession of almost 30 consecutive dry days that might have caused crops loss in part of the region. Therefore, farmers who lost their crops were forced to resow their lands after precipitation stabilized. Other than farmers who lost their first sowing, this pattern might also be related to farmers that waited until the stabilization of rains to start their sowing operation, with a smaller climatic risk.

The irrigated pixels sowing date median is 1 day after the rainy season onset (average of 3 days), even though, in recent years (after 2013), most pixels were sowed before rainy season onset (Figure 4 and Figure S7, Table 1). In particular, in years where rainy season is delayed, irrigated pixels sowing dates are less affected than rainfed pixels. In addition, in years that rainfed farmers are forced to resow after crop failure (two-peak sowing pattern in Figure 5), no second sowing peak is evident for irrigated lands, indicating resiliency through dry spells in the beginning of crop development.

The sowing of the irrigated second crop, on average, occurred 159 days following the onset of the rainy season, whereas the rainfed second crop occurs, on average, 20 days after irrigated pixels. Naturally, both in rainfed and irrigated pixels, a delay in irrigated first crop sowing results in later second crop sowing dates.

Rainfed first crop sowing dates are positively correlated to the rainy season onset, with an average correlation coefficient of 0.473 (and median of 0.510), whereas irrigated first crop sowing dates are weakly correlated to the rainy season, with an average and a median correlation coefficient of approximately 0.036 and 0.013, respectively (Table 2). These results indicate that rainfed systems are strongly dependent on rainy season onset to start the sowing operation, as expected, whereas irrigated farms can maintain sowing dates (or even advance them) even in years when the rainy season is delayed.

Table 2. Pearson correlation coefficient of rainy season onset and sowing dates in Western Bahia.

Sowing Dates			
First crop		Second crop	
Rainfed	Irrigated	Rainfed	Irrigated
0.473 (0.510)	0.036 (0.013)	−0.056 (−0.067)	−0.034 (−0.040)

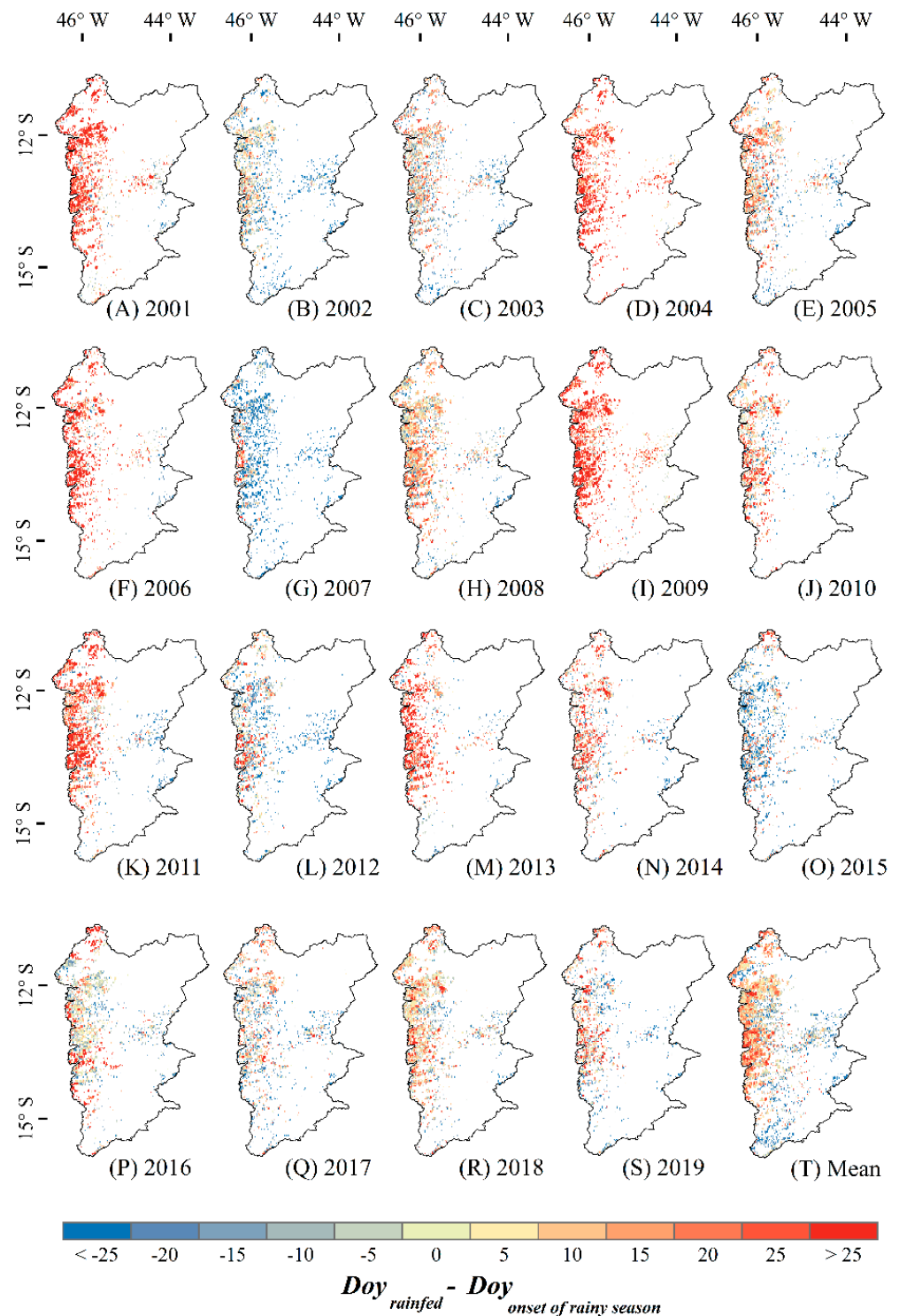


Figure 7. Spatial distribution of the difference between rainfed sowing dates and rainy season onset from 2001 to 2019 (A–S). Panel (T) shows the average anomaly for each pixel.

4. Discussion

The limited spatiotemporal information about sowing and harvest dates in Brazil is the main barrier to the large-scale assessment of the crop–climate relationship and how it determines the total output or viability of multiple cropping in the country [6,14]. By building a sowing calendar time series (from 2011 to 2019) in a high spatial resolution (~500 m), we fill this gap for a complex and dynamical area such as Western Bahia, with

the potential to expand to other regions. This historical sowing calendar allowed for the identification of how farmers of rainfed and irrigated farms have responded in abnormally dry years (when economic impacts are potentially high) and the modification of sowing patterns throughout time.

Our results show that the sowing operation in WB starts at the eastern part of the region (late September–early October) and follows to the west (late November–early December), in an east–west gradient. Rainy season onset, contrastingly, starts earlier in the west (early October) and later in the east (late November). This counterintuitive relationship is due to a combination of factors. First, phytosanitary measures to control Asian soybean rust (*Phakopsora pachyrhizi*) prevents soybean sowing (first crop) before October 15th in central and western WB [46], leaving early sowing restricted to the east of the municipalities of Luís Eduardo Magalhães, São Desidério, Barreiras and Correntina [21,46]. Second, other municipalities located in the eastern part of the region, such as Barra (sugar cane, beans and cassava), Canápolis (sugar cane, beans and cassava), Cristópolis (beans) and Feira da Graça (sugar cane, beans and cassava) cultivate crops that are not restricted by the phytosanitary regulations that affect soybean sowing [47], and sow in the beginning of October.

In addition, our analysis indicated that rainfed sowing dates are late, positively correlated to rainy season onset dates and are particularly affected in years where rains are delayed, but that was not the case for irrigated lands. For the latter, by the time rainy season starts, most of the pixels have already sown their crops, even in years where rains are delayed. Moreover, while no significant trend was detected in rainy season onset dates, irrigated lands are sowing earlier every year. Even though the possibility to sow early (even before rainy season onset) carries a higher hydrologic risk, it also brings many advantages. First, the water volume required for irrigation in the beginning of the cycle is small, as well as the energy costs. By the time the crop demands higher volumes of water (during grain filling, for example), rains are already consolidated in the region. Therefore, farmers might only irrigate again during a short period in the end of the second crop cycle, optimizing irrigation use in farms and saving energy costs. Second, because farmers make better use of the rainy season, they might even sow a third crop and cultivate five crops in 2 agricultural years. This ability increases the farms' income and preserves soil properties. Finally, early sowing also leads to advantages regarding phytosanitary diseases (soybean rust) because, by the time the fungus spreads in the abundant rainfed farms, crops in irrigated lands are already mature and close to harvesting. In that case, productivity levels are less affected and costs with pesticides are lower.

In addition to early sowing, irrigated farms sowing windows (both first and second crops) are shorter in the end than in the beginning of the study period and when compared to rainfed farms, regardless of the year analyzed. In addition, irrigated lands are more resilient to rainy season delays and avoid the “two-peak” seeding, as in 2007, when a small volume of rains prompted farmers to initiate the sowing operation (by the end of October), followed by a long dry spell (~30 days) that caused crop failure. Many rainfed farmers needed to resow their lands, with economical losses and impacts in crops productivity. This analysis indicates that irrigated farms have adapted their sowing operation towards a more intensive agriculture and efficient water use during the rainy season. In a scenario where the rainy season is projected to be frequently delayed in the next decades [48], this management practice could be an important adaptation strategy to keep high productivity levels.

However, the intense water use in the watersheds and the recent reduction in annual precipitation in the region might trigger water use conflicts, especially at the end of the dry season, when river flows are minimal [10]. In the transition months from dry to wet season, in addition to a lower available water volume, energy costs are higher, which could limit irrigation or increase products prices. Therefore, increasing the efficiency of the irrigation systems is also an important adaptation measure.

Indeed, severe droughts between 2012 and 2015 that hit Northeast Brazil were reflected in this study: during these years, rainy season onset occurred later than the region's historical average. Despite that, rainfed sowing dates were not delayed, probably because

precipitation in these years was still within acceptable standards for soybean seeding. Rains began on October 31st on average in 2012 and November 15th on average in 2015 (Figure 6). Even though sowing was not delayed, the region's grain production decreased by 35% in 2015 [42]. In contrast, irrigated pixels sowing took place up to twenty days before rained in 2015, even though the region experienced water conflicts [10], including the temporary suspension of water use concessions. During this period, the water table level of the Alto Grande basin, one of the most expressive in WB, also decreased by up to 5 m [9], indicating a potential increase in hydrological risk in the region.

In addition to the investigation of historical crop–climate relationships and how farmers responded in dry years, crop sowing date time series show important regional information that is crucial, especially for local government and policymakers, to support the future adaptation of multiple cropping systems in case predictions of increasingly extreme climate conditions are confirmed. In particular, sowing dates have been suggested as an important adaptation measure to maintain high yields in single or multiple cropping in regions where extreme climate conditions are increasing, especially longer dry seasons [8,14]. Indeed, our results strongly indicate that rained multiple cropping is particularly vulnerable to changes in rainy season onset (and rainy season length, since late sowing potentially inhibits the cultivation of a second crop) and, in case irrigation is not an option, would need to be based on diverse adaptation measures in a future drier climate, especially in WB, where the predominantly sandy soils show a high porosity and low water retention [49].

Finally, uncertainties and limitation of the results are related to: (i) the low availability of field data to perform a more robust validation of both management systems, perennial, or semi-perennial crops, as well as a third crop in irrigated lands; and (ii) the potential variation in NDVI behavior after green-up in the variety of crops cultivated in the region.

5. Conclusions

This is the first study that provided high spatial (~500 m) and temporal (yearly, from 2001 to 2019) maps of first and second crop calendars in Western Bahia, a complex area with continuous agricultural development, using a dense time series of vegetative indices. We were able to provide sowing dates for both rained and irrigated systems in the region. In addition, this is the first study that analyzes the rainy season onset–sowing dates relationship in a high spatiotemporal resolution in the region.

Our main findings are: (i) irrigated farms sow both first and second crops earlier and in a narrower window than rained; (ii) delays in rainy season onset affect first crop sowing dates in rained systems, but not in irrigated lands, which could sow up to 25 days before rains start in years of severe drought; (iii) delays in rainy season onset potentially causes a first sowing loss and subsequent resow in rained systems. In summary, irrigated lands show a stronger resilience in years where rains are delayed, and have adapted their sowing operation towards a more intensive agriculture and efficient water use during the rainy season. However, this resilience is threatened if the trend towards increasing water use and total precipitation reduction continues.

Finally, as recent climate projections indicate that the rainy season might be delayed more frequently in the future, double cropping farmers in Western Bahia could benefit from the investigation and investment in adaptation measures in order to maintain high productivity levels. Some of these measures include: hydrometeorological monitoring, rainy season onset and river flows forecast systems, more efficient irrigation systems and agroclimatological zoning.

Supplementary Materials: The following supporting information can be downloaded at: <https://www.mdpi.com/article/10.3390/agronomy12071679/s1>, Figure S1: Rainfed and irrigated croplands in Western Bahia from 2001 to 2019; Figure S2: Average Pearson correlation coefficient (A, B, C, D and E), its standard deviation (F, G, H, I and J); Nash–Sutcliffe model efficiency coefficient (K, L, M, N and O), and its standard deviation (P, Q, R, S and T) for each NDVI interpolation method; Figure S3: Percentage of cultivated area and Pearson’s correlation coefficient; Figure S4: Percentage of cultivated area and Nash–Sutcliffe model efficiency coefficient; Figure S5: Sowing dates of irrigated areas (first crop) in Western Bahia from 2001 to 2019; Figure S6: Sowing date of irrigated areas (second crop) in Western Bahia from 2001 to 2019; Figure S7: Spatial distribution of the difference between irrigated sowing dates and rainy season onset; Figure S8: Rainy season onset tendency (days.year⁻¹) and statistical significance ($\alpha = 5\%$). Table S1. Sowing interval for the main soybean (first crop) producing municipalities in Western Bahia. Planted soybean area (hectares and percentage) derived from the SIDRA platform. Mean \pm SD (DOY) are data obtained in this research. Sowing range (DOY) derived Portaria number 114, of 11 of May of 2021. Table S2. Observed and estimated sowing dates (DOY), and cultivated crops in each sampled center pivot in WB.

Author Contributions: Experimental design—G.F.P. and H.P.F.; data processing—H.P.F. and L.M.B.; manuscript writing—H.P.F.; review and editing—G.F.P. and L.M.B.; supervision—G.F.P.; project administration—G.F.P. All authors have read and agreed to the published version of the manuscript.

Funding: H.P.F. was supported by Conselho Nacional de Desenvolvimento Científico e Tecnológico (CNPq) (process: 130939/2019-6). This study was financed in part by the Coordenação de Aperfeiçoamento de Pessoal de Nível Superior—Brasil (CAPES)—Finance Code 001.

Institutional Review Board Statement: Not applicable.

Informed Consent Statement: Not applicable.

Data Availability Statement: Data are available upon request to the authors.

Acknowledgments: We thank Conselho Nacional de Desenvolvimento Científico e Tecnológico (CNPq) (process: 130939/2019-6) for the scholarship awarded to the first author and Coordenação de Aperfeiçoamento de Pessoal de Nível Superior—Brasil (CAPES).

Conflicts of Interest: The authors declare no conflict of interest.

References

1. CEPEA (Centro de Estudos Avançados em Economia Aplicada)—PIB do Agronegócio Brasileiro. 2021. Available online: <https://cepea.esalq.usp.br/br> (accessed on 27 May 2022).
2. Bragança, A. The Economic Consequences of the Agricultural Expansion in Matopiba. *Rev. Bras. Econ.* **2018**, *72*, 161–185. [[CrossRef](#)]
3. Dionizio, E.A.; Costa, M.H. Influence of Land Use and Land Cover on Hydraulic and Physical Soil Properties at the Cerrado Agricultural Frontier. *Agriculture* **2019**, *9*, 24. [[CrossRef](#)]
4. AIBA (Associação de Agricultores e Irrigantes da Bahia). Available online: <https://aiba.org.br/levantamento-de-safra/> (accessed on 27 May 2022).
5. Abrahão, G.M.; Costa, M.H. Evolution of Rain and Photoperiod Limitations on the Soybean Growing Season in Brazil: The Rise (and Possible Fall) of Double-Cropping Systems. *Agric. For. Meteorol.* **2018**, *256–257*, 32–45. [[CrossRef](#)]
6. Brumatti, L.M.; Pires, G.F.; Santos, A.B. Challenges to the Adaptation of Double Cropping Agricultural Systems in Brazil under Changes in Climate and Land Cover. *Atmosphere* **2020**, *11*, 1310. [[CrossRef](#)]
7. Pimenta, F.M.; Speroto, A.T.; Costa, M.H.; Dionizio, E.A. Historical Changes in Land Use and Suitability for Future Agriculture Expansion in Western Bahia, Brazil. *Remote Sens.* **2021**, *13*, 1088. [[CrossRef](#)]
8. Pires, G.F.; Abrahão, G.M.; Brumatti, L.M.; Oliveira, L.J.C.; Costa, M.H.; Liddicoat, S.; Kato, E.; Ladle, R.J. Increased Climate Risk in Brazilian Double Cropping Agriculture Systems: Implications for Land Use in Northern Brazil. *Agric. For. Meteorol.* **2016**, *228–229*, 286–298. [[CrossRef](#)]
9. Marques, E.A.G.; Silva Junior, G.C.; Eger, G.Z.S.; Ilambwetsi, A.M.; Raphael, P.; Generoso, T.N.; Oliveira, J.; Júnior, J.N. Analysis of Groundwater and River Stage Fluctuations and Their Relationship with Water Use and Climate Variation Effects on Alto Grande Watershed, Northeastern Brazil. *J. S. Am. Earth Sci.* **2020**, *103*, 102723. [[CrossRef](#)]
10. Pousa, R.; Costa, M.H.; Pimenta, F.M.; Fontes, V.C.; Castro, M. Climate Change and Intense Irrigation Growth in Western Bahia, Brazil: The Urgent Need for Hydroclimatic Monitoring. *Water* **2019**, *11*, 933. [[CrossRef](#)]
11. Butt, N.; De Oliveira, P.A.; Costa, M.H. Evidence That Deforestation Affects the Onset of the Rainy Season in Rondonia, Brazil. *J. Geophys. Res. Atmos.* **2011**, *116*, 2–9. [[CrossRef](#)]

12. Leite-Filho, A.T.; de Sousa Pontes, V.Y.; Costa, M.H. Effects of Deforestation on the Onset of the Rainy Season and the Duration of Dry Spells in Southern Amazonia. *J. Geophys. Res. Atmos.* **2019**, *124*, 5268–5281. [[CrossRef](#)]
13. Rodrigues, M.A.M.; Garcia, S.R.; Kayano, M.T.; Calheiros, A.J.P.; Andreoli, R.V. Onset and Demise Dates of the Rainy Season in the South American Monsoon Region: A Cluster Analysis Result. *Int. J. Climatol.* **2022**, *42*, 1354–1368. [[CrossRef](#)]
14. Zhang, M.; Abrahao, G.; Cohn, A.; Campolo, J.; Thompson, S. A MODIS-Based Scalable Remote Sensing Method to Estimate Sowing and Harvest Dates of Soybean Crops in Mato Grosso, Brazil. *Heliyon* **2021**, *7*, e07436. [[CrossRef](#)] [[PubMed](#)]
15. Boisier, J.P.; Ciaia, P.; Ducharne, A.; Guimberteau, M. Projected Strengthening of Amazonian Dry Season by Constrained Climate Model Simulations. *Nat. Clim. Chang.* **2015**, *5*, 656–660. [[CrossRef](#)]
16. Gao, F.; Anderson, M.C.; Zhang, X.; Yang, Z.; Alfieri, J.G.; Kustas, W.P.; Mueller, R.; Johnson, D.M.; Prueger, J.H. Toward Mapping Crop Progress at Field Scales through Fusion of Landsat and MODIS Imagery. *Remote Sens. Environ.* **2017**, *188*, 9–25. [[CrossRef](#)]
17. Nascimento Bendini, H.; Garcia Fonseca, L.M.; Schwieder, M.; Sehn Körting, T.; Rufin, P.; Del Arco Sanches, I.; Leitão, P.J.; Hostert, P. Detailed Agricultural Land Classification in the Brazilian Cerrado Based on Phenological Information from Dense Satellite Image Time Series. *Int. J. Appl. Earth Obs. Geoinf.* **2019**, *82*, 101872. [[CrossRef](#)]
18. Zeng, L.; Wardlow, B.D.; Wang, R.; Shan, J.; Tadesse, T.; Hayes, M.J.; Li, D. A Hybrid Approach for Detecting Corn and Soybean Phenology with Time-Series MODIS Data. *Remote Sens. Environ.* **2016**, *181*, 237–250. [[CrossRef](#)]
19. Funk, C.C.; Peterson, P.J.; Landsfeld, M.F.; Pedreros, D.H.; Verdin, J.P.; Rowland, J.D.; Romero, B.E.; Husak, G.J.; Michaelsen, J.C.; Verdin, A.P. A Quasi-Global Precipitation Time Series for Drought Monitoring. *U.S. Geol. Surv. Data Ser.* **2014**, *832*, 4.
20. Arvor, D.; Dubreuil, V.; Ronchail, J.; Simões, M.; Funatsu, B.M. Spatial Patterns of Rainfall Regimes Related to Levels of Double Cropping Agriculture Systems in Mato Grosso (Brazil). *Int. J. Climatol.* **2014**, *34*, 2622–2633. [[CrossRef](#)]
21. IBGE (Sistema IBGE de Recuperação Automática—Produção Agrícola Municipal: Tabela 5457—Área Plantada ou Destinada à Colheita, Área Colhida, Quantidade Produzida, Rendimento Médio e Valor da Produção das Lavouras Temporárias e Permanentes). Available online: <https://sidra.ibge.gov.br/tabela/5457> (accessed on 27 May 2022).
22. Zhong, L.; Hu, L.; Yu, L.; Gong, P.; Biging, G.S. Automated Mapping of Soybean and Corn Using Phenology. *ISPRS J. Photogramm. Remote Sens.* **2016**, *119*, 151–164. [[CrossRef](#)]
23. Schaaf, C.; Wang, Z. MCD43A4 MODIS/Terra+Aqua BRDF/Albedo Nadir BRF Adjusted Ref Daily L3 Global -500 m V006. *NASA EOSDIS Land Processes DAAC.* **2015**. [[CrossRef](#)]
24. Hsieh, P.F.; Lee, L.C.; Chen, N.Y. Effect of Spatial Resolution on Classification Errors of Pure and Mixed Pixels in Remote Sensing. *IEEE Trans. Geosci. Remote Sens.* **2001**, *39*, 2657–2663. [[CrossRef](#)]
25. Chen, J.; Jönsson, P.; Tamura, M.; Gu, Z.; Matsushita, B.; Eklundh, L. A Simple Method for Reconstructing a High-Quality NDVI Time-Series Data Set Based on the Savitzky-Golay Filter. *Remote Sens. Environ.* **2004**, *91*, 332–344. [[CrossRef](#)]
26. Beck, P.S.A.; Atzberger, C.; Høgda, K.A.; Johansen, B.; Skidmore, A.K. Improved Monitoring of Vegetation Dynamics at Very High Latitudes: A New Method Using MODIS NDVI. *Remote Sens. Environ.* **2006**, *100*, 321–334. [[CrossRef](#)]
27. Elmore, A.J.; Guinn, S.M.; Minsley, B.J.; Richardson, A.D. Landscape Controls on the Timing of Spring, Autumn, and Growing Season Length in Mid-Atlantic Forests. *Glob. Chang. Biol.* **2012**, *18*, 656–674. [[CrossRef](#)]
28. Gu, L.; Post, W.M.B.; Baldocchi, D.D.; Black, T.A.; Suyker, A.E.; Verma, S.B.; Vesala, T.; Wofsy, S.C. Characterizing the Seasonal Dynamics of Plant Community Photosynthesis Across a Range of Vegetation Types. In *Phenology of Ecosystem Processes: Applications in Global Change Research*, 1st ed.; Noormets, A., Ed.; Springer: New York, NY, USA, 2009; pp. 35–58.
29. Zhang, X.; Friedl, M.A.; Schaaf, C.B.; Strahler, A.H.; Hodges, J.C.F.; Gao, F.; Reed, B.C.; Huete, A. Monitoring Vegetation Phenology Using MODIS. *Remote Sens. Environ.* **2003**, *84*, 471–475. [[CrossRef](#)]
30. White, M.A.; de Beurs, K.M.; Didan, K.; Inouye, D.W.; Richardson, A.D.; Jensen, O.P.; O’Keefe, J.; Zhang, G.; Nemani, R.R.; van Leeuwen, W.J.D.; et al. Intercomparison, Interpretation, and Assessment of Spring Phenology in North America Estimated from Remote Sensing for 1982–2006. *Glob. Chang. Biol.* **2009**, *15*, 2335–2359. [[CrossRef](#)]
31. Diao, C. Remote Sensing Phenological Monitoring Framework to Characterize Corn and Soybean Physiological Growing Stages. *Remote Sens. Environ.* **2020**, *248*, 111960. [[CrossRef](#)]
32. Diao, C.; Li, G. Near-Surface and High-Resolution Satellite Time Series for Detecting Crop Phenology. *Remote Sens.* **2022**, *14*, 1957. [[CrossRef](#)]
33. Gao, F.; Zhang, X. Mapping Crop Phenology in Near Real-Time Using Satellite Remote Sensing: Challenges and Opportunities. *J. Remote Sens.* **2021**, *2021*, 8379391. [[CrossRef](#)]
34. Yang, Y.; Ren, W.; Tao, B.; Ji, L.; Liang, L.; Ruane, A.C.; Fisher, J.B.; Liu, J.; Sama, M.; Li, Z.; et al. Characterizing Spatiotemporal Patterns of Crop Phenology across North America during 2000–2016 Using Satellite Imagery and Agricultural Survey Data. *ISPRS J. Photogramm. Remote Sens.* **2020**, *170*, 156–173. [[CrossRef](#)]
35. Diao, C.; Yang, Z.; Gao, F.; Zhang, X.; Yang, Z. Hybrid Phenology Matching Model for Robust Crop Phenological Retrieval. *ISPRS J. Photogramm. Remote Sens.* **2021**, *181*, 308–326. [[CrossRef](#)]
36. Tan, B.; Morisette, J.; Wolfe, R.; Esaias, W.; Gao, F.; Ederer, G.; Nightingale, J.; Nickeson, J.E.; Ma, P.; Pedely, J. Modis Vegetation Phenology Metrics Estimated with an Enhanced Timesat Algorithm. *J. Sel. Top. Appl. Earth Obs. Remote Sens.* **2011**, *4*, 4.
37. Zhang, Q.; Kong, D.; Shi, P.; Singh, V.P.; Sun, P. Vegetation Phenology on the Qinghai-Tibetan Plateau and Its Response to Climate Change (1982–2013). *Agric. For. Meteorol.* **2018**, *248*, 408–417. [[CrossRef](#)]
38. Soltani, A.; Sinclair, T.R. *Modelling Physiology of Crop Development, Growth and Yield*; CABI: Wallingford, UK, 2012.

39. Santos, A.B.; Costa, M.H.; Mantovani, E.C.; Boninsenha, I.; Castro, M. A Remote Sensing Diagnosis of Water Use and Water Stress in a Region with Intense Irrigation Growth in Brazil. *Remote Sens.* **2020**, *12*, 3725. [[CrossRef](#)]
40. Liebmann, B.; Camargo, S.J.; Seth, A.; Marengo, J.A.; Carvalho, L.M.V.; Allured, D.; Fu, R.; Vera, C.S. Onset and End of the Rainy Season in South America in Observations and the ECHAM 4.5 Atmospheric General Circulation Model. *J. Clim.* **2007**, *20*, 2037–2050. [[CrossRef](#)]
41. Paredes-Trejo, F.J.; Barbosa, H.A.; Lakshmi Kumar, T.V. Validating CHIRPS-Based Satellite Precipitation Estimates in Northeast Brazil. *J. Arid Environ.* **2017**, *139*, 26–40. [[CrossRef](#)]
42. De Araújo, M.L.S.; Sano, E.E.; Bolfe, É.L.; Santos, J.R.N.; dos Santos, J.S.; Silva, F.B. Spatiotemporal Dynamics of Soybean Crop in the Matopiba Region, Brazil (1990–2015). *Land Use Policy* **2019**, *80*, 57–67. [[CrossRef](#)]
43. Reis, L.; Silva, C.M.S.E.; Bezerra, B.; Mutti, P.; Spyrides, M.H.; Silva, P.; Magalhães, T.; Ferreira, R.; Rodrigues, D.; Andrade, L. Influence of Climate Variability on Soybean Yield in Matopiba, Brazil. *Atmosphere* **2020**, *11*, 1130. [[CrossRef](#)]
44. CPTEC—CLIMANÁLISE: Boletim de Monitoramento de Análise Climática. São Paulo: SCT/INPE-CPTEC. Available online: <http://climanalise.cptec.inpe.br/~rclimanl/boletim/0904/index.html> (accessed on 27 May 2022).
45. Cunha, A.P.M.A.; Tomasella, J.; Ribeiro-Neto, G.G.; Brown, M.; Garcia, S.R.; Brito, S.B.; Carvalho, M.A. Changes in the Spatial–Temporal Patterns of Droughts in the Brazilian Northeast. *Atmos. Sci. Lett.* **2018**, *19*, 1–8. [[CrossRef](#)]
46. De Melo, A.C.A.; Nobre Júnior, A.D.A.; da Silva, F.A.M.; Abreu, L.M. de Zoneamento De Risco Climático Para Cultivo Da Soja No Cerrado. *Nativa* **2020**, *8*, 26. [[CrossRef](#)]
47. ADAB—Agência Estadual de Defesa Agropecuária da Bahia. Portaria No. 59, de 29 de Janeiro de 2009. Procedimentos para o Vazio Sanitário da Soja no Oeste da Bahia. Available online: <http://www.adab.ba.gov.br/modules/conteudo/conteudo.php?conteudo=16> (accessed on 27 May 2022).
48. Byrne, M.P.; Pendergrass, A.G.; Rapp, A.D.; Wodzicki, K.R. Response of the Intertropical Convergence Zone to Climate Change: Location, Width, and Strength. *Curr. Clim. Chang. Rep.* **2018**, *4*, 355–370. [[CrossRef](#)] [[PubMed](#)]
49. Campos, R.; Pires, G.F.; Costa, M.H. Soil Carbon Sequestration in Rainfed and Irrigated Production Systems in a New Brazilian Agricultural Frontier. *Agriculture* **2020**, *10*, 156. [[CrossRef](#)]